

A Test Procedure for Determining Models of LV Equipment

Vladimir Čuk, Joseph F. G. Cobben, Wil L. Kling, Roelof B. Timens, and Frank B. J. Leferink

Abstract—An automated test technique for determining parameters of low voltage equipment is presented in the paper. The aim of this research is to obtain simple models of household, office and industrial equipment which could be used to predict power quality problems during the design of low voltage installations and networks. For that purpose, several types of equipment were tested in the PQ laboratory and in this phase of the research, the emphasis is on inrush currents and interaction between voltage and currents during voltage changes (magnitude and harmonic content changes).

Index Terms—Power quality, modeling, measurement, harmonics, inrush current.

I. INTRODUCTION

LIMITATIONS for the supply voltage concerning power quality phenomena are described in the standard EN 50160 and national grid codes. These standards are applicable for normal operating conditions. On the other hand, the IEC 61000 series of standards give some guidance for determining immunity requirements for devices and large installations, but not in all situations because of some simplifying assumptions, such as idealized test conditions.

Abnormal network situations can be modeled and simulated with high accuracy in software such as Matlab, Digisilent Power Factory, Alternative Transients Program and other packages. These programs require a lot of experience and details about the models, which sometimes makes them inconvenient to use during the design of the installation.

This was the reason to start working on a tool which could give assistance for installation/network design, and prevent most of the possible power quality problems. To keep the tool user friendly, the tool should not need too many details about all of the future components.

This is one of the tasks of the recently started IOP project: Power Quality and EMC which involves Eindhoven University of Technology and University of Twente. One of the starting points of this project is model development. Models should be physically based as much as possible, but some of the model parameters should be avoided in order to achieve greater simplicity during the installation design.

V. Čuk, J. F. G. Cobben, and W. L. Kling are with Eindhoven University of Technology, Eindhoven, Netherlands (e-mail: v.cuk@tue.nl).

R. B. Timens and F. B. J. Leferink are with the University of Twente, Enschede, Netherlands.

Model simplifications can be obtained through experiments, as described in the following sections, and statistical analysis of the results. This cannot be achieved for all types of equipment, but it still offers a convenient way of modeling a large number of equipment. For example, different types of office equipment, which can come in a large number, it is unnecessary to model all equipment with too much detail. The models could also include some widespread immunity limits, and therefore pinpoint some of the possible problematic locations in the installation.

II. EXPERIMENTAL SETUP

The experimental setup for this automated procedure is schematically shown in Fig. 1.

The voltage source used in these experiments is the California Instruments MX 45, a 3 phase source with maximal apparent power of 45 kVA, maximal voltage of 300 V (phase to ground), and programmable up to the 50th harmonic. It is programmed from the PC (in Matlab) via RS232 connection, as suggested by [1] and [2].

Loads are connected to the voltage source by compliance impedances suggested by the IEC725 standard which is equal to $(0.40+j\cdot0.25) \Omega$ for phase and neutral in total. Loads can be connected separately or in parallel, in one or three phases.

Signals are measured with a Tiepie Engineering HS3 oscilloscope, with 2 channels and resolution of 16 bits. At the moment, this is enough for one phase connection, but it can be expanded for three phase measurement in the future. The

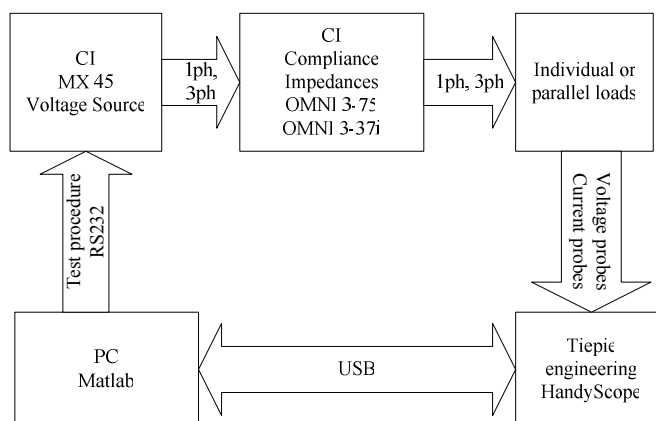


Fig. 1. Schematic diagram of the laboratory setup.

oscilloscope is connected to the PC by a USB connection, and is also controlled from Matlab.

III. SOFTWARE AND EXPERIMENTS

The software is completely developed in Matlab, Release 2008b. It is capable to produce input voltage waveforms and record voltage and current signals at the load connection. The structure of software execution is briefly described in Fig. 2.

Multiple tests can be created by this way, and the laboratory setup can complete them autonomously and store all of the results on the PC for post processing.

First of the tests conducted is the inrush current test. It is described in the next section. Also, interaction of voltages and currents during the presence of harmonic disturbances was measured and analyzed, as an expansion of the harmonic fingerprints, described in [3] and [4].

IV. THE INRUSH CURRENT TEST

Inrush currents of devices can cause several power quality problems. Fast voltage variations are caused by inrushes, and their impact sometimes has to be limited [5]. This is especially the case if the installation is powered by an uninterruptible power supply. In that case, equipment selection is influenced by inrush conditions even more [6].

If the equipment is working in a regime which requires constant turning on and off, inrush currents can cause flickering effect in the nearby lighting.

In some cases, inrush currents can cause unwanted tripping (unwanted protection reactions) [7]. For this reason it is important to know the inrush characteristic before protection is selected and set.

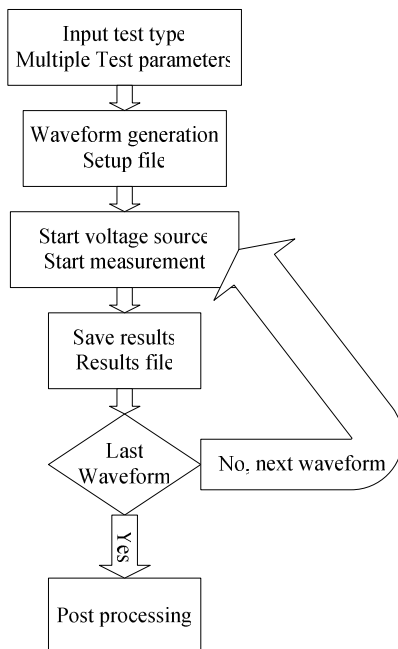


Fig. 2. Simplified execution diagram of the software.

The inrush current test consists of a series of equipment starts at different voltage phase angles, and measurements of voltage and current. For every voltage phase angle a number of repetitions can be set, in order to check the validity of results by comparing them with other results for the same starting phase.

The phase range of 360° can be divided in any number of intervals. In the results presented here, the range was divided in 24 intervals, giving a phase step of 15° . For every phase angle 3 repetitions were chosen, and deviations from the average value were calculated for all characteristics.

The test was conducted on an air inductor of 50 mH with active resistance of 3.2Ω , and on a vacuum cleaner with electronic speed control. The speed reference of the vacuum cleaner was set to roughly one half of the maximal speed.

One measured sample of the starting voltage waveform is given in Fig. 3, with the starting phase set to 90° .

A sample of the measured inrush current waveform for the 50 mH inductor is given in Fig. 4. The starting voltage phase was set to 90° .

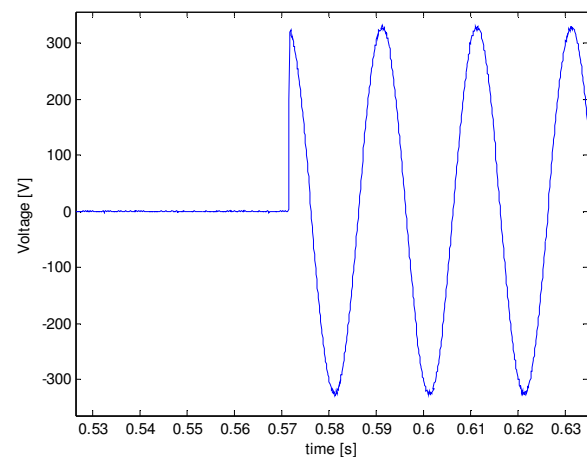


Fig. 3. Sample of the measured starting voltage.

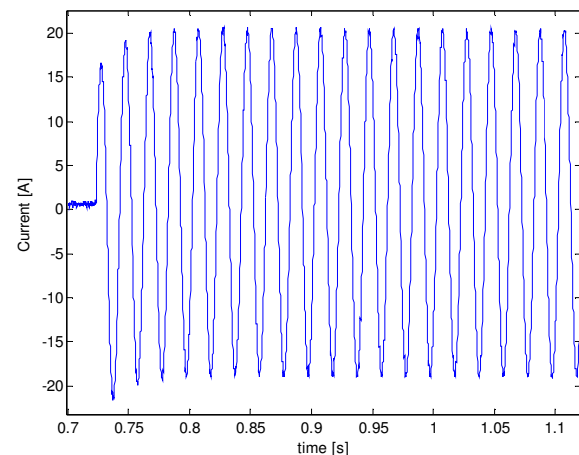


Fig. 4. Inrush current sample – 50 mH inductor.

A sample of the measured inrush current waveform for the vacuum cleaner is given in Fig. 5. The starting voltage phase was set to 90° .

The dependence of the inductors maximal inrush current (peak of the waveform) from the starting voltage phase is presented in Fig. 6. Maximal current values from Fig. 6 are average values from repetitions of that phase angle. Maximal deviations of repetitions from those average values are given in Fig. 7. It can be seen on Fig. 7 that these deviations are relatively small, as a consequence of accurate source phase triggering.

The dependence of the maximal value of the inductors DC current component from the starting voltage phase is given in Fig. 8. By comparing Fig. 6 and Fig. 8 it can be seen that the maximum of the inrush current depends mostly on its DC component, which in turn is largely dependent on voltage starting phase as an initial condition (as it was expected for an inductor).

In the case of the vacuum cleaner with electronic speed control, these dependencies cannot be explained as easy as for

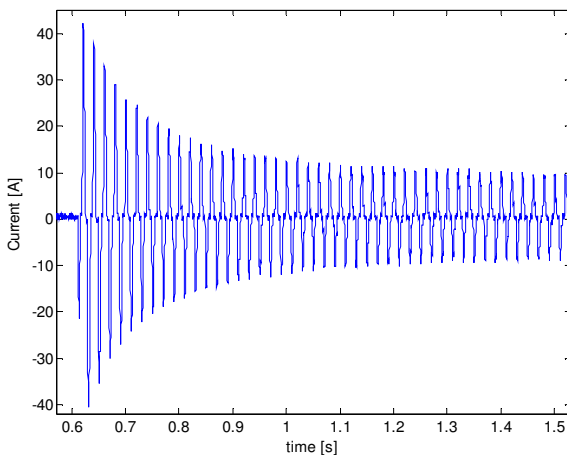


Fig. 5. Inrush current sample – vacuum cleaner.

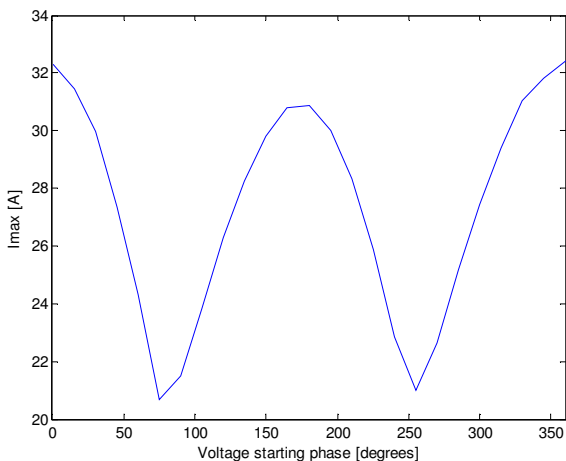


Fig. 6. Dependence of inductors maximal peak inrush current value from the voltage starting phase.

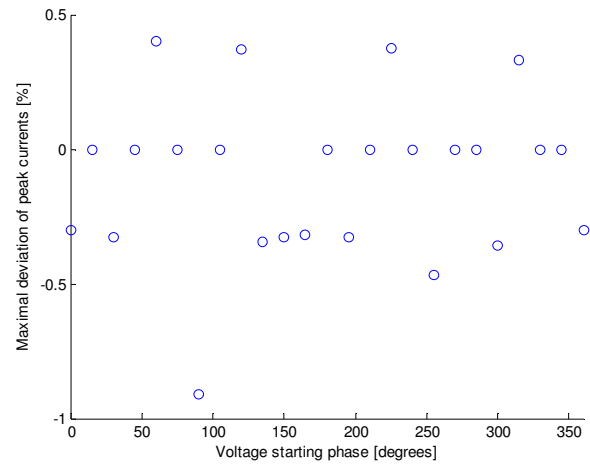


Fig. 7. Maximal deviations of inductors peak currents among repetitions.

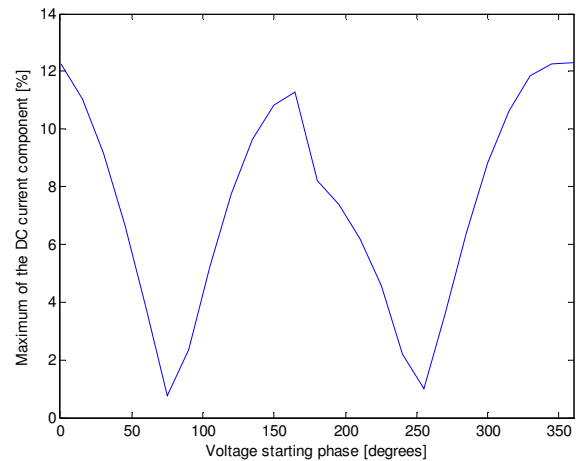


Fig. 8. Dependence of inductors maximal DC current component from the voltage starting phase.

the inductor. The reason for that is unknown topology of the converter used.

The dependence of the vacuum cleaners maximal starting current from the starting voltage phase is given in Fig. 9. Maximal deviations of repetitions from the average values in Fig. 9 are presented in Fig. 10. It can be seen that the deviations are approximately two times bigger than in the case of the inductor. That can be explained by a higher sensitivity of the inrush current to voltage phase changes.

Random switching of devices gives an even value of probability for any voltage starting phase angle. By exploring the angle distribution of inrush characteristics it is possible to predict the inrush properties with a certain level of probability. Doing so, smaller rated values of other installation components (for example fuses) can be selected in some cases. This can be used to avoid extreme values which could be highly unlikely to appear, as suggested in [8] for a ferroresonant regulated rectifier.

From the inrush currents measured, some characteristic values were calculated as presented in Table I.

In Table I, following abbreviations are used: I_{\max} is the

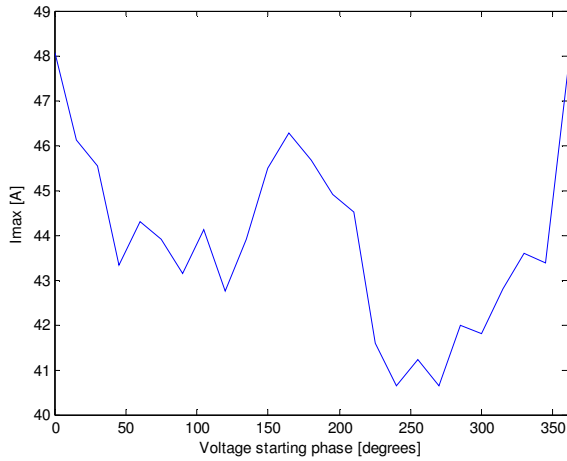


Fig. 9. Dependence of vacuum cleaners maximal inrush current from the voltage starting phase.

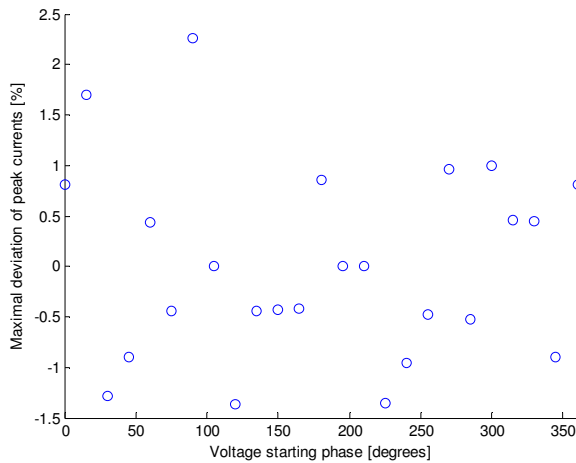


Fig. 10. Maximal deviations of vacuum cleaners peak currents among repetitions.

absolute maximal value of current for all measurements, $I_{\max 90\%}$ is the maximal value of current for 90% of the measurements, $I_{DC\max}$ is the absolute maximal value of the DC current component, $I_{DC\max 90\%}$ is the maximal DC current component value for 90% of the measurements, $t_{in\max}$ is the maximal inrush duration for all measurements, and $t_{in\max 90\%}$ is the maximal inrush duration for 90% of the measurements.

From Table I it can be seen that for these two devices 90% probability values are very close to absolute maximal values.

V. THE HARMONIC FINGERPRINT TEST WITH MULTIPLE HARMONICS

Harmonic fingerprinting is a method which describes the interaction between the distorted supply voltage and the harmonic current of a device or a whole installation. The whole procedure and test results for several types of equipment are described in details in [3] and [4]. One application of this test procedure – tracing the levels of grid and installation impact on the overall current distortion is described in [9].

TABLE I
CHARACTERISTICS INRUSH CURRENT VALUES

	50 mH Inductor	Vacuum cleaner
I_{\max} [A]	32.4	48.5
$I_{\max 90\%}$ [A]	31.8	46.3
$I_{DC\max}$ [A]	12.3	5.59
$I_{DC\max 90\%}$ [A]	12.2	4.31
$t_{in\max}$ [s]	0.24	1.37
$t_{in\max 90\%}$ [s]	0.22	1.20

In short, the test procedure is done as follows. At first, the load tested is connected to an undistorted voltage. At that time, the loads current spectrum without background harmonic voltage is recorded. After that, harmonic voltages are added to the supply voltage with equidistant magnitude and phase steps, and voltages, currents, and their spectra's are recorded. With all of the measurements done, it is possible to make a load model for every harmonic frequency. Harmonic models consists of a harmonic current source (harmonic currents recorded with undistorted source voltage) in parallel with a harmonic impedance (calculated from the harmonic voltage and harmonic currents measured with and without voltage distortion).

For an approximately linear load, each harmonic impedance can have a single complex value. For loads with strong nonlinear behavior, impedances can be used as look up tables, with different impedance values for different harmonic voltage magnitudes and phase stands.

If a harmonic fingerprint is made for a single load, the results can be used to calculate harmonic currents of several parallel loads with one harmonic voltage applied. The currents calculated will match well with values measured for parallel loads, as reported in [3] and [4].

For the test presented here, model parameters were calculated for the 5th and 11th harmonic, and impedances were saved as look up tables. Voltage amplitude step was 2% of the nominal voltage, in the range from 2 to 10%. Voltage phase step used was 60°. The test was done on two devices, one with a liner behavior – a 25 W fan, and one with an extremely nonlinear behavior – an energy saving lamp.

Harmonic voltages applied for the calculation of the 5th harmonic impedances are presented in the complex plain in Fig. 11. Measured 5th harmonic currents for the fan and energy saving lamp used in complex plain are given in Fig. 12 and Fig. 13, respectively.

From Fig. 13 it can be seen that for the energy saving lamp there is a strong connection between the harmonic voltage phase and the resulting harmonic current, which justifies the usage of an impedance look up table instead of a linearized value. For the fan a single impedance value could be used, but for the sake of comparison again a look up table was used.

After the model calculation, a test was done with the 5th and the 11th harmonic voltage applied at the same time. The level of 11th harmonic was kept constant with a magnitude of 3% and phase stand of 120°, and the 5th harmonic was changed from 2 to 5% with magnitude steps of 1% and phase steps of 60°.

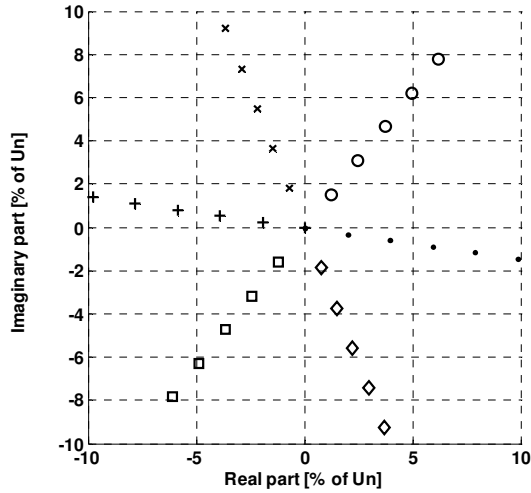


Fig. 11. Voltage values used in the test – 5th harmonic.

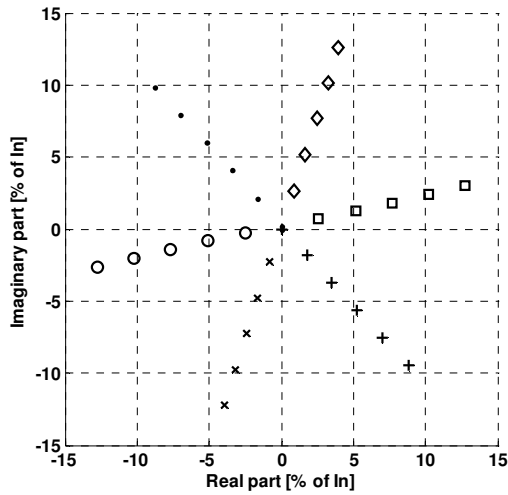


Fig. 12. Measured 5th harmonic current – fan.

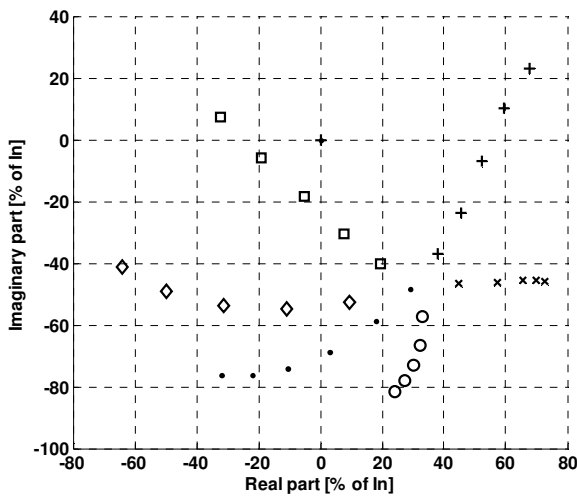


Fig. 13. Measured 5th harmonic current – ES lamp.

currents were compared to the values calculated from the model obtained with single harmonic measurements. Relative calculation errors for the fan are given in Fig. 14, and for the energy saving lamp in Fig. 15.

From Fig. 14 and Fig. 15 it is obvious that the calculation is much more accurate for a mostly linear device. Also, it is noticeable that the accuracy of the calculation for the energy saving lamp is improving as the magnitude of the harmonic voltage increases (voltage magnitude is increasing with the number of measurement). One partial reason for that is the measurement accuracy for small values. Another, more important reason, is the effect of the constant harmonic in the background. For a nonlinear device, the existence of the 11th harmonic can cause a significant amount of the 5th harmonic by itself. In case of the fan, cross talk ratio for 11th harmonic (the ratio of the 11th current harmonic and the second biggest harmonic caused when only the 11th voltage harmonic is applied) is 50. In the case of the energy saving lamp, this ratio is only 1.1.

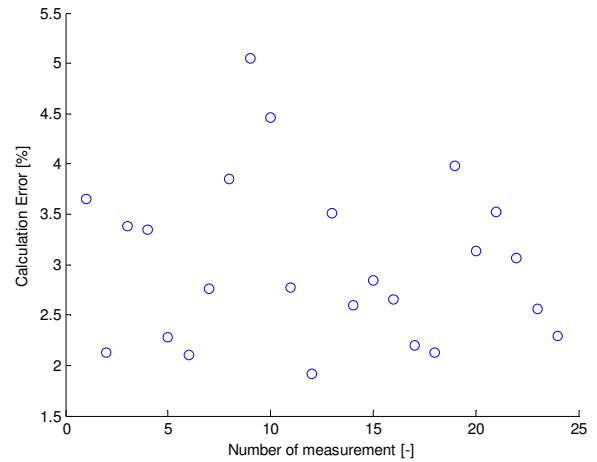


Fig. 14. Relative calculation error – fan, 5th harmonic.

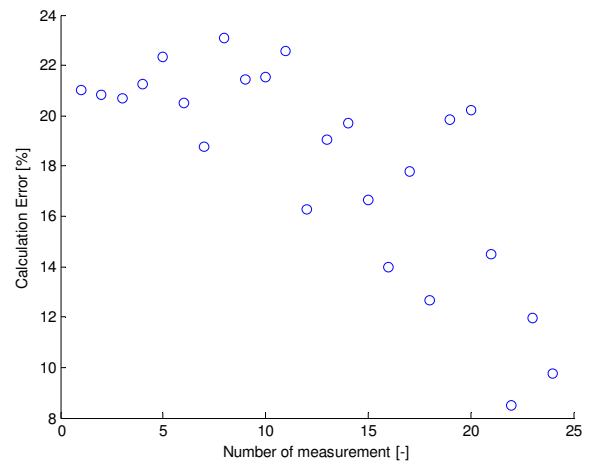


Fig. 15. Relative calculation error – ES lamp, 5th harmonic.

After the measurement, values of 5th and 11th harmonic

VI. CONCLUSIONS

Inrush characteristics of devices can be treated statistically to find the most probable values. However, in cases like the two analyzed, they can be very close to the maximal values possible.

Complete frequency decoupling in harmonic modeling gives good results when the elements are mostly linear or when the voltage distortion is mostly composed of one harmonic. With total nonlinearity and complex voltage distortions some level of frequency coupling is needed, and will be explored further.

REFERENCES

- [1] California instruments: MX Series, SCPI programming manual, Revision R, July 2007.
- [2] S.E. Lyshevski, "Engineering and scientific computations using MATLAB," John Wiley & Sons, 2003.
- [3] A.J. Bosman, J.F. Cobben, W.L. Kling, J.M. Myrzik, "Harmonic modeling of solar inverters and their interaction with distribution grid," UPEC Newcastle, United Kingdom, September 2006.
- [4] J.F. Cobben, W.L. Kling, J.M. Myrzik, "The Making and purpose of harmonic fingerprints," CIRED Vienna, Austria, May 2007.
- [5] M. Nagpal, T.G. Martinich, A. Moshref, K. Morison, P. Kundur, "Assessing and limiting of transformer inrush current on power quality," IEEE Transactions on Power Delivery, Vol. 21, No. 2, April 2006.
- [6] V. Zaltsman, "Inrush current control for equipment powered by UPSs," INTELEC '89 Conference Proceedings, pp. 19.4/1-19.4/7, Vol. 2, October 1989.
- [7] D. Jiandong, W. Chang, Y. Jianming, "Study of the inrush current identification using the improved half-cycle Fourier analysis," APPEEC 2009, Asia-Pacific Power and Energy Conference, March 2009.
- [8] T.M. Vega, W.W. Burns, "A probabilistic study of inrush currents in a ferroresonant regulated rectifier," INTELEC '78 Conference Proceedings, pp. 374-383, October 1978.
- [9] J. Casteren, J.F. Cobben, "Harmonics: Harmonizing a shared Responsibility," CIRED Vienna, Austria, May 2007.